ARTICLE TEMPLATE

A photoelectron imaging and quantum chemistry study of the deprotonated cyan fluorescent protein chromophore anion

Michael A. Parkes, Anabel Bennett and Helen H. Fielding[a]

[a]Department of Chemistry, University College London, 20 Gordon Street, London, WC1H 0AJ

ARTICLE HISTORY
Compiled March 27, 2019

ABSTRACT
Cyan fluorescent protein (CFP), a blue-shifted analogue of green fluorescent protein, is used widely as a fluorescence resonance energy transfer donor in live cell fluorescence imaging. Here, we use a combination of anion photoelectron spectroscopy experiments and quantum chemistry calculations to probe the electronic structure of the CFP chromophore in its deprotonated anionic form. The vertical detachment energy measured as the maximum in the photoelectron spectrum is 2.75 ± 0.02 eV, which is an improvement on our earlier measurement. We see evidence for competing internal conversion following resonant excitation of electronically excited states of the anion lying in the detachment continuum. We find that the first electronically excited valence state of the anion lies very close to the detachment threshold, supporting the conclusions of gas-phase photodestruction action spectroscopy measurements, and that the second electronically excited valence state lies around 1.25 eV above the detachment threshold. These electronic states have shape resonance character and mixed excited shape and Feshbach resonance character, respectively.

KEYWORDS
Anion photoelectron spectroscopy; autodetachment; fluorescent proteins; photochemistry; photophysics

1. Introduction

Green fluorescent protein (GFP), and its family of variants, have revolutionised many areas of the life sciences by enabling *in vivo* monitoring of biological and biochemical processes [1–5]. The chromophore that lies at the heart of GFP is formed by intramolecular cyclisation of a serine-tyrosine-glycine sequence, at positions 65-67 of the protein, and it is localised in the centre of a β-barrel structure. The chromophore exists in neutral and anionic (deprotonated) forms which have different hydrogen-bond networks around the phenolic oxygen on the tyrosine residue and different spectral properties. The anionic form absorbs light around 480 nm and fluoresces around 508 nm with a high quantum yield ($\Phi \sim 0.8$) [6]. The neutral form absorbs light around 395 nm, after which it can undergo ultrafast excited state proton transfer to form the deprotonated anionic form of the chromophore which then fluoresces around 508 nm.

One way to change the fluorescence wavelength is to replace the tyrosine residue at position 66 with a different amino acid residue. Substituting tyrosine with tryptophan

CONTACT H. H. Fielding. Email: h.h.fielding@ucl.ac.uk

has been shown to give rise to blue-shifted cyan fluorescent proteins (CFPs) [7, 8] that have proved valuable for applications requiring multicolour imaging and fluorescence resonance energy transfer (FRET). Tryptophan residues do not usually exist in their deprotonated forms in biological systems because of the high pK_a of the indole unit ($\sim$ 20); however, it has been shown that it is possible to modify the microenvironment of the chromophore to support deprotonation of the indole group (Fig. 1) and form a CFP in which the chromophore exists in its deprotonated anionic form [9]. Although CFPs continue to play an important role in biological imaging, the electronic structure of the deprotonated CFP chromophore anion is still relatively unexplored compared to that of the deprotonated GFP chromophore anion.

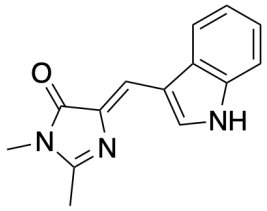

Figure 1. Structure of the CFP chromophore.

Experimentally, a direct way of determining the electronic structure of deprotonated protein chromophore anions is to use electrospray-ionisation anion photoelectron spectroscopy [10]. Measuring the electron binding energies of the isolated CFP chromophore in its deprotonated anionic form in the gas phase, free from interactions with the protein environment, allows the intrinsic electronic structure of the chromophore to be determined in detail and provides access to the higher lying electronically excited states of the chromophore that cannot be measured easily in a native protein environment because the UV absorption of the chromophore overlaps with that of aromatic amino acid residues.

Gas-phase photodestruction action spectroscopy measurements using the electrostatic heavy ion storage ring at Aarhus (ELISA) had a maximum around 456 nm (2.72 eV) for the deprotonated CFP chromophore anion [11]. In earlier work, we reported vertical detachment energies of 2.9 $\pm$ 0.1 eV and 4.0 $\pm$ 0.1 eV and found evidence to suggest that, at higher photon energies, autodetachment from an excited electronic state of the chromophore anion comptetes with electron detachment [12]. Here, we report the results of a new, combined photoelectron spectroscopy and computational chemistry study of the deprotonated CFP chromophore anion. We report a more precise value for the VDE to the ground electronic state of the neutral deprotonated radical and we report excitation energies and resonance characters of the first two electronically excited singlet states of the deprotonated CFP chromophore anion.

2. Methods

2.1. Experimental

Photoelectron spectra were recorded using our electrospray ionization (ESI) velocity map imaging (VMI) spectrometer that has been described elsewhere [13]. Briefly, anions were generated from a ($\sim$1 mM) solution of the CFP chromophore dissolved in methanol with a few drops of aqueous ammonia added to aid deprotonation. Anions

from the ESI are mass-selected by a quadrupole mass filter, guided into a hexapole ion trap filled with helium and subsequently released from the trap at 20 Hz (for experiments employing nanosecond laser pulses) or 250 Hz (for experiments employing femtosecond laser pulses) and focused into the source region of a collinear VMI spectrometer. Nanosecond laser pulses of wavelength $352 - 310$ nm are generated by frequency-doubling the output of a nanosecond YAG-pumped dye laser operating at 20 Hz. Femtosecond laser pulses of wavelength 400 nm are generated by frequency-doubling the output of an amplified Ti:Sapphire femtosecond laser system operating at 250 Hz.

Photoelectrons generated in the source region of the VMI spectrometer are accelerated towards a position sensitive detector and imaged by a CCD camera. Laser only images are recorded without the ion-beam and subtracted from the overall signal to remove background electron counts arising from ionisation of residual gas or scattered laser light. The resulting photoelectron images were inverted using the pBASEX method to obtain photoelectron velocity and angular distributions [14]. Electron kinetic energy (eKE) spectra were obtained by calibrating the radial photoelectron velocity distribution against the photoelectron spectrum of iodide ($352 - 310$ nm) or indole (400 nm) [15]. The energy resolution is $\Delta E/E \sim 4\%$ and error bars for peak maxima are quoted as ± 0.02 eV based on the the error associated with selecting peak maxima being ± 1 pixel of the CCD camera.

2.2. Computational

The structures of the various conformers of the deprotonated CFP chromophore anion and their corresponding neutral radicals were optimised using density functional theory (DFT) with the CAM-B3LYP [16–20] functional and the aug-cc-pVDZ [21] basis set. Frequency calculations were performed to confirm that minima in the potential energy surfaces were reached.

Vertical detachment energies (VDEs) were calculated using various methods. We used DFT to calculate the VDE as the energy difference between the anion and neutral radical at the optimised geometry of the anion using CAM-B3LYP and ωB97X-D [22] functionals. We used the electron propagator theory (EPT) method with the outer valence Greens function (OVGF) propagator [23–25]. We also used the equation-of-motion coupled-cluster method with single and double excitations for the calculation of ionisation potentials (EOM-IP-CCSD) [26]. The adiabatic detachment energy was determined as the energy difference between the anion and neutral radical in their ground vibrational states. We have found these methods to give reasonable agreement with experiment for other protein chromophore anions and their building blocks [15, 27–35].

Vertical excitation energies (VEEs) of the excited singlet states of the anions were calculated using the ADC(2) method [36, 37], with the 6-31+G* basis set [38–40]. This approach has been shown to compare favourably with high level methods for other protein chromophores [30, 33, 35]. The excited states above the detachment threshold contain continuum states and to account for the interaction of resonance states with the continuum, a basis set with diffuse functions is necessary. The size of the basis set determines the number of continuum states that are calculated. The 6-31+G* basis set was a compromise between size and computational expense. We note that an alternative approach could be to use CAP-EOM-CC [41].

Geometry optimisations, vibrational frequencies and EPT calculations were per-

formed using the Gaussian09 software suite [42] and EOM-IP-CCSD and ADC(2) calculations were carried out using the Q-Chem software package [43].

Photoelectron spectra were calculated using ezSpectrum (version 3.0) [44]. This calculation requires the equilibrium geometries, harmonic frequencies and normal mode vectors of the conformers of the deprotonated CFP chromophore anion and their corresponding neutral radicals as input and we used those obtained using the CAM-B3LYP/aug-cc-pVDZ method. The Franck-Condon overlap integrals were calculated using the parallel normal mode approximation. The vibrational temperature of the anions is assumed to be around 300 K and the minimum intensity threshold was set to 0.001. The maximum number of vibrational quanta in the anion and neutral radicals were limite to 2 (anion) and 4 (neutral radical). The resulting stick spectra were convoluted with Gaussian instrument profiles with full-width at half maximum (FWHM) values equivalent to an instrumental resolution of $\Delta E/E = 4\%$.

3. Results

There are four possible stereoisomers of the deprotonated CFP chromophore anion with *cis* and *trans* conformations about the exocyclic double bond and *cis* and *trans* conformations about the exocyclic single bond (Fig. 1). The CAM-B3LYP/aug-cc-pVDZ optimised geometries and relative energies of the four stereoisomers are shown in Fig. 2. In our earlier work, NMR measurements of the CFP chromophore in methanol-d_4 solution revealed the presence of isomers with *cis* and *trans* conformations about the double bond; both of these isomers had a *trans* configuration about the exocyclic C-C single bond. The *cis-trans* and *trans-trans* CFP chromophores existed in an 8.2:1 ratio, favouring the *cis-trans* isomer. Thus, we believe that our anion beam will be composed predominantly of *cis-trans* and *trans-trans* deprotonated CFP chromophore anions.

Photoelectron spectra of the deprotonated CFP chromophore anion were recorded as a function of eKE and are plotted in Fig. 3. The spectra are also presented as a function of electron binding energy (eBE = $h\nu$ − eKE). The photoelectron angular distributions were isotropic (Supplementary Information).

All the photoelectron spectra have similar profiles: a broad feature at low eBE (high eKE, defined as eKE > 0.2 eV) and a sharp feature at high eBE (low eKE, defined as eKE < 0.2 eV). The broad features at low eBE have sharp rising edges with maxima that remain at constant eBE (2.75 ± 0.02 eV) with increasing photon energy, signifying that this feature arises from direct detachment to the D_0 continuum. The peak maxima are very close to the calculated VDEs (Table 1) and shifted towards lower eBE than our earlier measurement (2.9 ± 0.1 eV) which was obtained from a poorer resolution photoelectron spectrum [12]. The broad features at low eBE appear to broaden out towards higher eBE at higher photon energies, typical of an indirect detachment process via an electronically excited state of the anion embedded in the detachment continuum. We do not see evidence of direct detachment to D_1, but this lies higher in energy (Table 1).

The high eBE (low eKE) regions of the photoelectron spectra are very similar in shape and position (eKE) for all wavelengths in the range 400 − 310 nm, signifying that they arise from an indirect detachment process such as autodetachment from a low-lying electronically excited state lying close to the detachment threshold or from vibrational autodetachment or thermionic emission from vibrationally hot S_0 populated by internal conversion from higher lying electronically excited states.

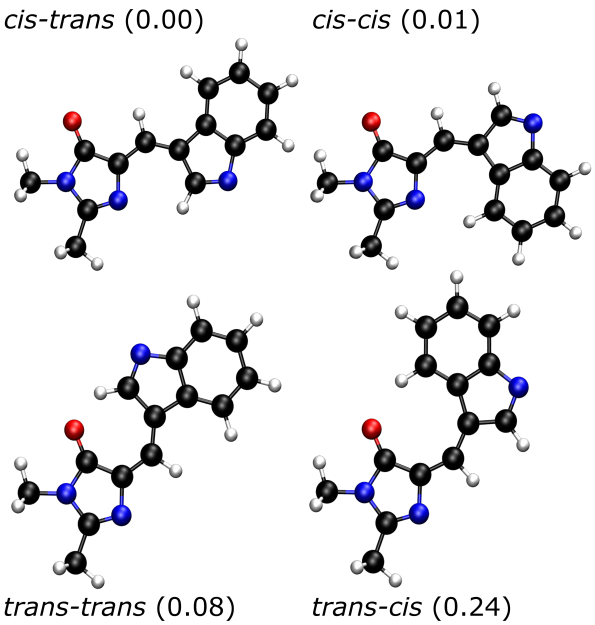

Figure 2. Stereoisomers of the deprotonated CFP chromophore anion; the first *cis*/*trans* label refers to the exocyclic double bond (adjacent to the imidazolinone group) and the second *cis*/*trans* label refers to the exocyclic single bond (adjacent to the deprotonated indole group). CAM-B3LYP/aug-cc-pVDZ calculated relative energies (in eV) are also shown.

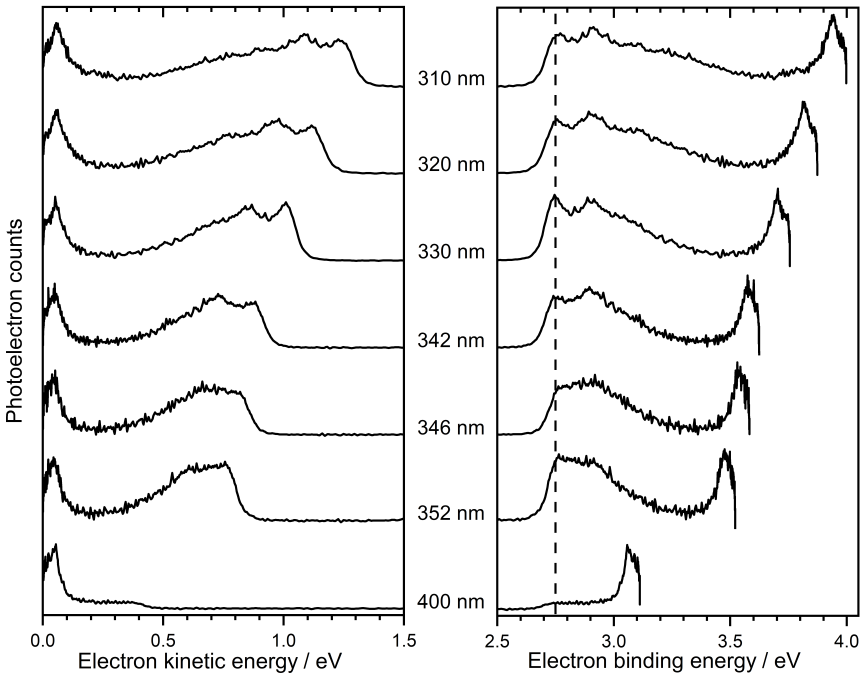

Figure 3. Photoelectron spectra of deprotonated CFP at wavelengths of 400 nm (3.10 eV), 352 nm (3.52 eV), 346 nm (3.58 eV), 342 nm (3.63 eV), 330 nm (3.76 eV), 320 nm (3.87 eV) and 310 nm (4.00 eV) plotted as a function of electron kinetic energy (eKE) and electron binding energy (eBE). The experimental VDE is taken as the top of the peak in the 330 nm photoelectron spectrum and is marked with a dashed vertical line.

Table 1. Calculated vertical detachment energies (VDEs) for $S_0 - D_0$ and $S_0 - D_1$ processes in deprotonated *cis-trans* and *trans-trans* CFP chromophores compared with the maximum of the low eBE peak in the 330 nm experimental spectrum. The values in parentheses are ADEs (0-0 transitions). All calculations employed the aug-cc-pVDZ basis set and all values are in eV.

		D_0	D_1
CAM-B3LYP	*cis-trans*	2.81 (2.67)	
	trans-trans	2.81 (2.68)	
ωB97X-D	*cis-trans*	2.80	
	trans-trans	2.80	
EPT	*cis-trans*	2.63	4.11
	trans-trans	2.62	4.10
EOM-IP-CCSD	*cis-trans*	2.67	4.14
	trans-trans	2.68	4.13
Experiment		2.75 ± 0.02	4.0 ± 0.1 [12]

The eKE distribution of electrons emitted by thermionic emission from the vibrationally hot ground state of an anion, $P(\epsilon)$, has been shown to be modelled well by Klots' formula [45, 46],

$$P(\epsilon) \propto \epsilon^{1/2} \exp(-\epsilon / k_B T_{M\cdot}), \tag{1}$$

where k_B is Boltzmann's constant and $T_{M\cdot}$ is the temperature of the resulting neutral radical [47–49],

$$T_{M\cdot} = T_{M^-} + (h\nu - \mathrm{ADE})/C_v. \tag{2}$$

T_{M^-} is the initial temperature of the anions before photoexcitation, C_v is the microcanonical heat capacity. The microcanonical heat capacity $C_v \approx C_{canonical} - k_B \approx C_{canonical}$, since the heat capacities are $\sim 10^{-3}$ eV K^{-1}. Using the CAM-B3LYP/aug-cc-pVDZ ADE for the *cis-trans* isomer, estimations of $C_{canonical}$ from our quantum chemistry calculations (2.469×10^{-3} eV K^{-1}) and assuming $T_{M^-} = 298$ K, $T_{M\cdot}$ may be estimated as 476 K for the lowest energy *cis-trans* isomer. The modelled thermionic emission curve is presented in Fig. 4 together with the low eKE components of the photoelectron spectra.

The modelled thermionic emission curve fits reasonably well to the low eKE edge of the photoelectron spectra and to the overall exponential decay; however, there is an additional sharp peak centered around 0.05 eV eKE. The observation of a sharp peak at low eKE that does not change with photon energy suggests a vibration-mediated detachment process from an electronically excited state of the anion lying close to the detachment threshold.

To identify the excited electronic states of the anion that could be accessible following photoexcitation in the range 400−310 nm (3.10−4.00 eV), we calculated the VEEs, oscillator strengths and main configurations of the valence excited states of the *cis-trans* and *trans-trans* conformers of the deprotonated CFP chromophore anion. The results of these calculations are summarised in Table 2 and illustrated schematically in Fig. 5. Time-dependent DFT (TD-DFT) calculations of the VEEs, oscillator strengths and main configurations gave states with similar main configurations (Supplementary

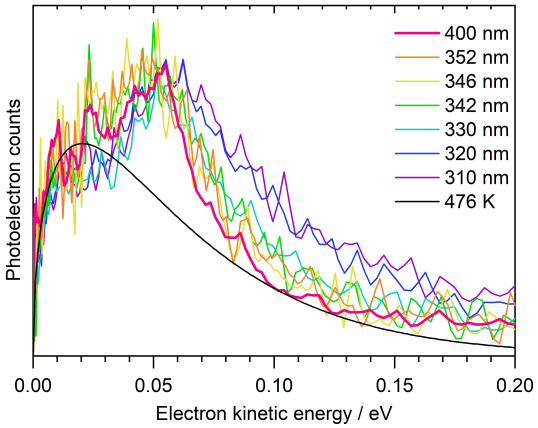

Figure 4. Photoelectron spectra of the CFP chromophore anion for eKE ≤ 0.2 eV following photoexcitation in the range $400 - 310$ nm. The solid black line is the modelled thermionic emission curve using Klots' formula at 476 K (see text). The spectra have been scaled to align their rising edges.

Information).

Table 2. ADC(2)/6-31+G* calculated vertical excitation energies (VEEs) of the lowest two singlet states of the deprotonated CFP chromophore anions with non-negligible oscillator strengths, f. All values are in eV.

		VEE (f)	Main configuration
S_1	*cis-trans*	2.87 (1.06)	$0.62(\pi_{63} \rightarrow \pi^*_{70})$
	trans-trans	2.93 (0.99)	$0.62(\pi_{63} \rightarrow \pi^*_{71})$
S_2	*cis-trans*	4.02 (0.01)	$-0.41(\pi_{63} \rightarrow \pi^*_{76}) + 0.30(\pi_{62} \rightarrow \pi^*_{70})$
	trans-trans	4.02 (0.02)	$-0.44(\pi_{63} \rightarrow \pi^*_{77}) + 0.31(\pi_{62} \rightarrow \pi^*_{71})$

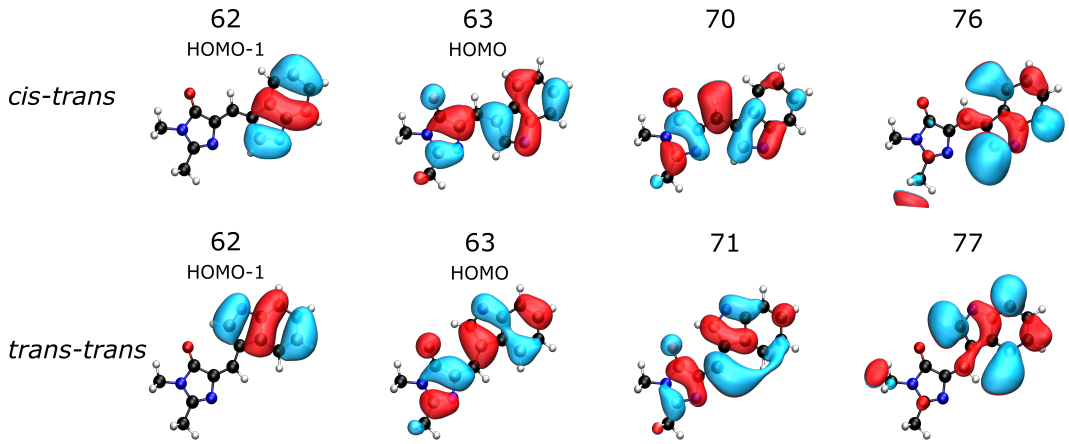

Figure 5. ADC(2)/6-31+G* molecular orbitals of the *cis-trans* (top) and *trans-trans* (bottom) isomers of the deprotonated CFP chromophore anion.

An excited state of $\pi\pi^*$ character and high oscillator strength is found at around 2.9 eV (430 nm), close to the reported maximum in photodestruction action spectroscopy measurements (2.72 eV) [11] and the measured D_0 VDE (Fig. 3 and Table

1). Excitation of this state involves a $\pi_{\mathrm{HOMO}} \rightarrow \pi^*$ transition and so this state has shape resonance character with respect to the D_0 continuum, which would be consistent with autodetachment following direct photoexcitation of S_1 at 400 nm (3.10 eV). A higher lying excited state of $\pi\pi^*$ character and non-negligible oscillator strength is found at around 4 eV (310 nm). Excitation of this state involves a mixture of $\pi_{\mathrm{HOMO}} \rightarrow \pi^*$ and $\pi_{\mathrm{HOMO-1}} \rightarrow \pi^*$ transitions and so this state can be considered as having both excited-shape and Feshbach resonance character with respect to the D_0 continuum.

To assist with our interpretation of the shapes of the photoelectron spectra, we calculated the photoelectron spectrum corresponding to direct photodetachment from the S_0 state of the deprotonated CFP chromophore anion to the D_0 state of the neutral radical. The calculated stick spectrum is presented in Fig. 6 together with the stick spectrum convoluted with a Gaussian instrument function with FWHM $\Delta E/E = 4\%$ and the 330 nm experimental photoelectron spectrum. The 330 nm spectrum was selected because the first peak is most clearly resolved in this spectrum. The most intense line in the stick spectrum is the 0-0 transition which is calculated at the CAM-B3LYP/aug-cc-pVDZ level to lie at 2.67 eV (the calculated spectrum in Fig. 6 has been shifted by 0.07 eV to provide the best fit to the rising edge of the experimental spectrum). The rest of the photoelectron spectrum is dominated by out-of-plane vibrations of the carbon and nitrogen skeleton. We attribute the difference between the simulated and experimental spectra at higher eBE to be largely the result of indirect detachment from a higher lying electronically excited state; the calculated VEE of the second $\pi\pi^*$ state is around 4 eV, which is just above the photon energy (3.76 eV). This second $\pi\pi^*$ state has some excited-shape resonance character with respect to the D_0 detachment continuum, so the electronic coupling between S_2 and the D_0 continuum is expected to be strong and autodetachment can therefore be relatively fast.

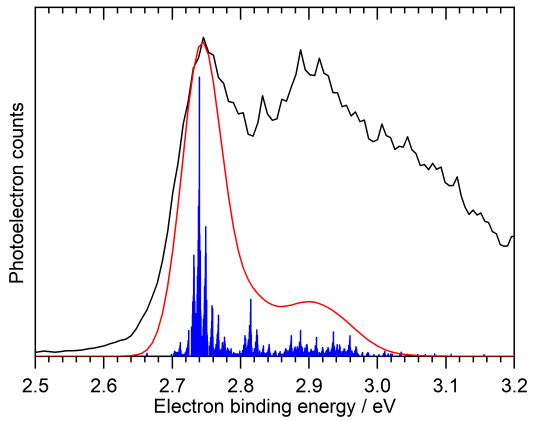

Figure 6. Calculated $S_0 - D_0$ stick spectrum at 300 K for the deprotonated CFP chromophore anion in its lowest energy *cis-trans* conformation (blue) with the calculated stick spectrum convoluted with an instrument function (red solid line) and experimental photoelectron spectrum following photoexcitation at 330 nm (black solid line).

4. Discussion

The VDE to the ground electronic state of the deprotonated CFP chromophore anion, D_0, was measured to be 2.75 $\pm$ 0.02 eV, which is an improvement on our earlier measurement of 2.9 $\pm$ 0.1 eV [12]. In order to understand the indirect photodetachment processes contributing to the broadening of the photoelectron spectra of the deprotonated CFP chromophore anion, following photoexcitation in the range 346 – 310 nm, and the feature at high eBE (low eKE), following photoexcitation in the range 400 – 310 nm, it is useful to consider the relative energies of the states involved and their electronic characters (Table 2). The energy level structure is illustrated schematically in Fig. 7.

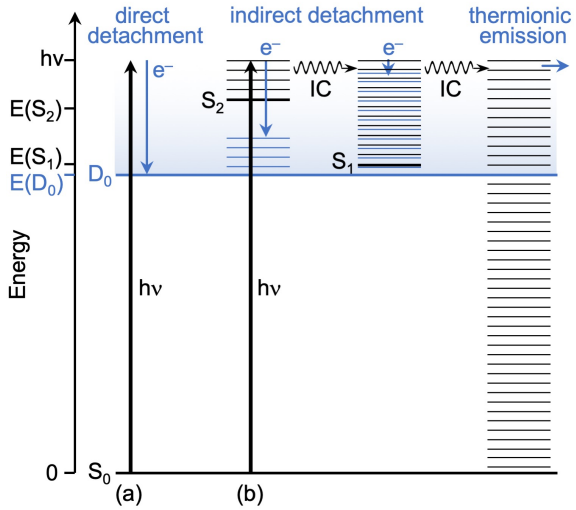

Figure 7. Schematic energy level diagram illustrating the possible electron detachment processes following photoexcitation of the deprotonated CFP chromophore anion. Thin horizontal black lines represent the vibrational levels of the electronic states of the anion and the blue shaded area represents the electron detachment continuum. Vertical blue arrows represent the eKE of direct and indirect electron detachment processes and the thin horizontal blue lines represent the vibrational energy left in the neutral radical following electron detachment (determined by the propensity for conservation of vibrational energy). The horizontal black arrow represents internal conversion (IC). (a) Direct photodetachment from S_0 to the D_0 continuum. (b) Indirect photodetachment processes following photoexcitation of S_2 with excess vibrational energy, $E_v = h\nu - E(S_2)$.

Resonant photoexcitation of S_1 (400 nm) and S_2 (352 - 310 nm) compete with direct detachment. Following photoexcitation of S_2, vibration-electronic coupling between S_2 and D_0 results in autodetachment (observed as a broadening of the low eBE feature towards high eBE) and vibration-electronic coupling between S_2 and S_1 or S_0 results in internal conversion back to S_1 or the electronic ground state. Following population of S_1 (either directly by photoexcitation at 400 nm or indirectly by internal conversion from S_2), vibration-electronic coupling between S_1 and D_0 may result in autodetachment (observed as a sharp peak at 0.05 eV eKE) and vibration-electronic coupling between S_1 and S_0 may result in competing internal conversion back to the electronic ground state. If high lying vibrational levels of S_0 are populated by internal conversion from S_1, vibration-electronic coupling between the ground electronic states of the anion and neutral radical may result in vibrational autodetachment [50]. Alternatively, coupling between the high density of vibrational states in S_0 may result in statistical redistribution of vibrational energy and delayed emission of electrons with an eKE

profile defined by Eq. (1).

The profile of the low eKE component of all the photoelectron spectra has a component that could be attributed to thermionic emission, as well as a sharp peak centered around 0.05 eV that we attribute to a vibration-mediated detachment process. Vibration-mediated detachment from S_1 would be consistent with our measurement of the detachment threshold lying close to the maximum in the photodestruction action spectroscopy measurement of the deprotonated CFP anion (2.72 eV) [11]. However, it is worth noting that the electric dipole moment of the *cis-trans* neutral radical is around 5.1 D, which is high enough to support a dipole-bound state [51]. Vibration-mediated autodetachment has been observed from resonantly excited dipole bound states of deprotonated phenolate anions [52, 53] and from dipole bound states that have been populated following internal conversion from valence excited states [54]. To determine whether the sharp peak at 0.05 eV eKE is attributed to vibration-mediated detachment from S_1 or from a dipole-bound state will require high-resolution photoelectron spectroscopy measurements and high-level quantum chemistry calculations.

Our original motivation for this work was to compare the electronic structure of the isolated deprotonated CFP chromophore with that of the isolated GFP chromophore. The VDEs of the two chromophore anions are similar: 2.73 - 2.8 eV for the GFP chromophore anion [12, 55–57] and 2.75 ± 0.02 eV for the CFP chromophore anion. The first electronically excited state in each chromophore involves a HOMO $\rightarrow \pi^*$ transition that lies very close to the detachment threshold. Action absorption spectroscopy measurements of the deprotonated CFP chromophore led to the conclusion that the VEE lies around 2.7 eV. The most recent action absorption measurements of the deprotonated GFP chromophore anion give a value of 2.75 eV for the VEE and 2.53 eV for the AEE [58], placing the origin of S_1 below the detachment threshold and the VEE very close to the detachment threshold. Our ADC(2) calculations suggest that the next $\pi\pi^*$ state in the deprotonated CFP chromophore has mixed Feshbach and excited shape resonance character with respect to the D_0 continuum and lies around 4 eV. In the deprotonated GFP chromophore, high level calculations predict two $\pi\pi^*$ states lying very close together at 3.74 eV and 3.78 eV, one with mostly Feshbach resonance character and the other with mostly excited-shape resonance character, with respect to the D_0 continuum [32]. Thus, the overall pattern of energy levels is very similar for the two chromophore anions.

A noteworthy difference between the photoelectron spectra of the two chromophore anions following excitation of the higher lying states is the existence of a more significant low eKE signal for the CFP chromophore anion (Figs 3 and 4) compared to the GFP chromophore anion [32, 55, 56], signifying that nuclear dynamics and internal conversion compete more effectively with autodetachment in the CFP chromophore. It has been proposed that the excited shape resonance in the GFP chromophore acts as an electron gateway state for resonant electron transfer from the deprotonated chromophore [32]. Thus, it seems that resonant electron transfer from the deprotonated CFP chromophore would be less efficient than resonant electron transfer from the deprotonated GFP chromophore.

5. Summary

The VDE of the deprotonated CFP chromophore measured as the maximum in the photoelectron spectrum has been determined to be 2.75 ± 0.02 eV. This is an improvement on our earlier measurement [12]. Following photoexcitation in the range

400 - 310 nm, we see evidence for resonant autodetachment and internal conversion to the ground electronic state. Our calculations show that the first electronically $\pi\pi^*$ state lies very close to the detachment threshold, in agreement with action absorption measurements [11], and has shape resonance character with respect to the detachment continuum. The next $\pi\pi^*$ state lies around 4 eV and has mixed excited shape resonance and Feshbach resonance character. Improving our understanding of the electronic structure of isolated photoactive protein chromophores in the gas-phase is a step towards first principles design of photoactive protein chromophores with specific characteristics.

Acknowledgements

The corresponding author is dedicating this paper to Professor Tim Softley to thank him for his encouragement and support and for providing her with the best possible start to her career. We acknowledge financial support from the EPSRC (EP/L005646/1) and the Royal Society and Leverhulme Trust (SRF\R1\180079). We are grateful to Dr Richard Fitzmaurice for synthesising the CFP chromophore, Professor Graham Worth for advice on the computational chemistry calculations and Dr Frank Otto for computational support.

Disclosure statement

There are no conflicts of interest.

Funding

This work was supported by EPSRC (EP/L005646/1) and the Royal Society and Leverhulme Trust (SRF\R1\180079).

References

[1] R.Y. Tsien, Annu. Rev. Biochem. **67** (1), 509–544 (1998).
[2] M. Zimmer, Chem. Rev. **102** (3), 759–782 (2002).
[3] S.R. Meech, Chem. Soc. Rev. **38** (10), 2922–2934 (2009).
[4] A.S. Mishin, V.V. Belousov, K.M. Solntsev and K.A. Lukyanov, Curr. Opin. Chem. Biol. **27**, 1–9 (2015).
[5] A. Acharya, A.M. Bogdanov, B.L. Grigorenko, K.B. Bravaya, A.V. Nemukhin, K.A. Lukyanov and A.I. Krylov, Chem. Rev. **117**, 758–795 (2017).
[6] A. Usman, O.F. Mohammed, E.T.J. Nibbering, J. Dong, K.M. Solntsev and L.M. Tolbert, J. Am. Chem. Soc. **127**, 11214–11215 (2005).
[7] R. Heim, D.C. Prashert and R.Y. Tsien, Proc. Natl. Acad. Sci. USA **91**, 12501–12504 (1994).
[8] A. Cubitt, L. Woollenweber and R. Heim, in *Green Fluorescent Proteins*, edited by Sullivan, K.F. and Kay, S.A., *Methods in Cell Biol.*, Vol. 58 (, , 1999), pp. 19–30.
[9] K.S. Sarkisyan, I.V. Yampolsky, K.M. Solntsev, S.A. Lukyanov, K.A. Lukyanov and A.S. Mishin, Scientific Reports **2**, 608 (2012).
[10] A. Henley and H.H. Fielding, Int. Rev. Phys. Chem. p. 10.1080/0144235X.2018.1548807 (2019).

[11] S. Boy, I.B. Nielsen, S.B. Nielsen, H. Krogh, A. Lapierre, H.B. Pedersen, S.U. Pedersen, U.V. Pedersen and L.H. Andersen, J. Chem. Phys. **119** (1), 338–345 (2003).
[12] C.R.S. Mooney, M.E. Sanz, A.R. McKay, R.J. Fitzmaurice, A.E. Aliev, S. Caddick and H.H. Fielding, J. Phys. Chem. A **116**, 7943–7949 (2012).
[13] A.R. McKay, M.E. Sanz, C.R.S. Mooney, R.S. Minns, E.M. Gill and H.H. Fielding, Rev. Sci. Instum. **81**, 123101 (2010).
[14] G.A. Garcia, L. Nahon and I. Powis, Rev. Sci. Instrum. **75** (11), 4989 (2004).
[15] M.A. Parkes, J. Crellin, A. Henley and H.H. Fielding, Phys. Chem. Chem. Phys. **20**, 15543–15549 (2018).
[16] A.D. Becke, J. Chem. Phys. **98**, 5648–5652 (1993).
[17] C. Lee, W. Yang and R.G. Parr, Phys. Rev. B **37**, 785–789 (1988).
[18] S.H. Vosko, L. Wilk and M. Nusair, Can. J. Phys. **58**, 1200–1211 (1980).
[19] P.J. Stephens, F.J. Devlin, C.F. Chabalowski and M.J. Frisch, J. Phys. Chem. **98**, 11623–11627 (1994).
[20] T. Yanai, D.P. Tew and N.C. Handy, Chem. Phys. Lett. **393** (1), 51 – 57 (2004).
[21] R.A. Kendall, T.H. Dunning Jr. and R.J. Harrison, J. Chem. Phys. **96** (May 2013), 6796–6806 (1992).
[22] J.D. Chai and M. Head-Gordon, Phys. Chem. Chem. Phys. **10** (44), 6615–6620 (2008).
[23] J. Linderberg and Y. Öhrn, *Propagators in Quantum Chemistry* (John Wiley & Sons, Inc., Hoboken, NJ, USA, 2004), p. 79.
[24] V.G. Zakrzewski, O. Dolgounitcheva, A.V. Zakjevskii and J.V. Ortiz, Annu. Rep. Comput. Chem. **6**, 79–94 (2010).
[25] J.V. Ortiz, WIREs Comput. Mol. Sci. **3**, 123–142 (2013).
[26] P.U. Manohar and A.I. Krylov, J. Chem. Phys. **129** (19), 194105 (2008).
[27] C. Mooney, M. Parkes, L. Zhang, H. Hailes, A. Simperler, M. Bearpark and H. Fielding, J. Chem. Phys. **140**, 205103 (2014).
[28] C. Mooney, M. Parkes, A. Iskra and H. Fielding, Angew. Chemie Int. Ed. **54**, 5646 –5649 (2015).
[29] M.A. Parkes, C. Phillips, M.J. Porter and H.H. Fielding, Phys. Chem. Chem. Phys. **18**, 10329–10336 (2016).
[30] C. McLaughlin, M. Assmann, M.A. Parkes, J.L. Woodhouse, R. Lewin, H.C. Hailes, G.A. Worth and H.H. Fielding, Chem. Sci. **8**, 1621–1630 (2017).
[31] J. Tay, M.A. Parkes, K. Addison, Y. Chan, L. Zhang, H.C. Hailes, P.C. Bulman Page, S.R. Meech, L. Blancafort and H.H. Fielding, J. Phys. Chem. Lett. **8**, 765–771 (2017).
[32] A.V. Bochenkova, C.R.S. Mooney, M.A. Parkes, J.L. Woodhouse, L. Zhang, R. Lewin, J.M. Ward, H.C. Hailes, L.H. Andersen and H.H. Fielding, Chem. Sci. **8**, 3154–3163 (2017).
[33] A. Henley, M. Diveky, A. Patel, M.A. Parkes, J.C. Anderson and H. Fielding, Phys. Chem. Chem. Phys. **19**, 31572–31580 (2017).
[34] J.L. Woodhouse, M. Assmann, M.A. Parkes, H. Grounds, S.J. Pacman, J.C. Anderson, G.A. Worth and H.H. Fielding, Phys. Chem. Chem. Phys. **19**, 22711–22720 (2017).
[35] A. Henley, A.M. Patel, M.A. Parkes, J.C. Anderson and H.H. Fielding, J. Phys. Chem. A **122**, 8222–8228 (2018).
[36] J. Schirmer, Phys. Rev. A **26** (5), 2395–2416 (1982).
[37] A.B. Trofimov and J. Schirmer, J. Phys. B At. Mol. Opt. Phys. **28**, 2299–2324 (1995).
[38] R. Krishnan, J.S. Binkley, R. Seeger and J.A. Pople, J. Chem. Phys. **72** (1), 650–654 (1980).
[39] T. Clark, J. Chandrasekhar, G.W. Spitznagel and P.V.R. Schleyer, J. Comput. Chem. **4** (3), 294–301 (1983).
[40] M.J. Frisch, J.A. Pople and J.S. Binkley, J. Chem. Phys. **80** (7), 3265–3269 (1984).
[41] T.C. Jagau, K.B. Bravaya and A.I. Krylov, Annu. Rev. Phys. Chem. **68**, 525–553 (2017).
[42] M.J. Frisch, G.W. Trucks, H.B. Schlegel, G.E. Scuseria, M.A. Robb, J.R. Cheeseman, G. Scalmani, V. Barone, B. Mennucci, G.A. Petersson, H. Nakatsuji, M. Caricato, X. Li, H.P. Hratchian, A.F. Izmaylov, J. Bloino, G. Zheng, J.L. Sonnenberg, M. Hada, M.

Ehara, K. Toyota, R. Fukuda, J. Hasegawa, M. Ishida, T. Nakajima, Y. Honda, O. Kitao, H. Nakai, T. Vreven, J.A. Montgomery, J.E. Peralta, F. Ogliaro, M. Bearpark, J.J. Heyd, E. Brothers, K.N. Kudin, V.N. Staroverov, R. Kobayashi, J. Normand, K. Raghavachari, A. Rendell, J.C. Burant, S.S. Iyengar, J. Tomasi, M. Cossi, N. Rega, J.M. Millam, M. Klene, J.E. Knox, J.B. Cross, V. Bakken, C. Adamo, J. Jaramillo, R. Gomperts, R.E. Stratmann, O. Yazyev, A.J. Austin, R. Cammi, C. Pomelli, J.W. Ochterski, R.L. Martin, K. Morokuma, V.G. Zakrzewski, G.A. Voth, P. Salvador, J.J. Dannenberg, S. Dapprich, A.D. Daniels, Ö. Farkas, J.B. Foresman, J.V. Ortiz, J. Cioslowski and D.J. Fox, Gaussian 09, Revision D.01 2009.

[43] Y. Shao, Z. Gan, E. Epifanovsky *et al.*, Advances in Molecular Quantum Chemistry Contained in the Q-Chem 4 Program Package 2015. <http://dx.doi.org/10.1080/00268976.2014.952696>.

[44] V. Mozhayskiy and A. Krylov, ezSpectrum . <http://iopenshell.usc.edu/downloads>.

[45] C.E. Klots, J. Chem. Phys. **98** (2), 1110–1115 (1993).

[46] C.E. Klots, J. Chem. Phys. **100** (2), 1035–1039 (1994).

[47] R. Mabbs, E. Surber and A. Sanov, Analyst **128** (6), 765–772 (2003).

[48] J.B. Wills, F. Pagliarulo, B. Baguenard, F. Lépine and C. Bordas, Chem. Phys. Lett. **390** (1-3), 145–150 (2004).

[49] B. Climen, F. Pagliarulo, A. Ollagnier, B. Baguenard, B. Concina, M.A. Lebeault, F. Lépine and C. Bordas, Eur. Phys. J. D **43** (1-3), 85–89 (2007).

[50] C.L. Adams, H. Schneider and J.M. Weber, J. Phys. Chem. A **114**, 4017–4030 (2010).

[51] J. Simons, J. Phys. Chem. A **112**, 6401–6511 (2008).

[52] H.T. Liu, C.G. Ning, D.L. Huang, P.D. Dau and L.S. Wang, Angew. Chemie Int. Ed. **52**, 8976–8979 (2013).

[53] D.L. Huang, H.T. Liu, C.G. Ning and L.S. Wang, J. Chem. Phys. **142**, 124309 (2015).

[54] J.N. Bull, C.W. West and J.R.R. Verlet, Phys. Chem. Chem. Phys. **17**, 32464–32471 (2015).

[55] D.A. Horke and J.R.R. Verlet, Phys. Chem. Chem. Phys. **14** (24), 8511–8515 (2012).

[56] Y. Toker, D.B. Rahbek, B. Klærke, A.V. Bochenkova and L.H. Andersen, Phys. Rev. Lett. **109** (12), 128101 (2012).

[57] S.H.M. Deng, X.Y. Kong, G. Zhang, Y. Yang, W.J. Zheng, Z.R. Sun, D.Q. Zhang and X.B. Wang, J. Phys. Chem. Lett. **5**, 2155–2159 (2014).

[58] H.V. Kiefer, H.B. Pedersen, A.V. Bochenkova and L.H. Andersen, Phys. Rev. Lett. **117** (24), 243004 (2016).